

Characteristics of biomass burning emission sources, transport, and chemical speciation in enhanced springtime tropospheric ozone profile over Hong Kong

C. Y. Chan,¹ L. Y. Chan,¹ J. M. Harris,² S. J. Oltmans,² D. R. Blake,³ Y. Qin,⁴ Y. G. Zheng,⁴ and X. D. Zheng⁵

Received 3 December 2001; revised 9 July 2002; accepted 15 July 2002; published 9 January 2003.

[1] Tropospheric ozone (O_3) enhancements have been continuously observed over Hong Kong. We studied the O_3 enhancement events and assessed their relation to the springtime O_3 maximum in the lower troposphere over Hong Kong using a 6-year (1993 to 1999) ozonesonde data set. We identified the source regions of biomass burning emission, and established the chemical and transport characteristics of O_3 -rich air masses in the enhanced O_3 profiles using satellite imagery, air trajectory and trace gas data measured on board the DC-8 aircraft during the PEM-West-B experiment. We identified a total of 39 O_3 enhancement events, among which 35 events (90%) occurred from late February to May and 30 events (77%) had O_3 enhancement within the 2.0–6.0 km altitude. The excess O_3 in the O_3 -rich layers adds an additional 12% of O_3 into the tropospheric O_3 column and results in an overall springtime O_3 maximum in the lower troposphere. Forward trajectory analysis suggests that the O_3 -rich air masses over Hong Kong can reach central Pacific and the western coast of North America within 10 days. Back air trajectories show that the O_3 -rich air masses in the enhanced profiles pass over the Southeast (SE) Asia subcontinent, where active biomass burning occurs in the O_3 enhancement period. We identified the Indo-Burma region containing Burma, Laos and northern Thailand, and the Indian-Nepal region containing northern India and Nepal as the two most active regions of biomass burning emissions in the SE Asia subcontinent. Ozone and trace gas measurement on board the DC-8 aircraft revealed that O_3 -rich air masses are found over many parts of the tropical SE Asia and subtropical western Pacific regions and they have similar chemical characteristics. The accompanying trace gas measurements suggest that the O_3 -rich air masses are rich in biomass burning tracer, CH_3Cl , but not the general urban emission tracers. We thus believe that the springtime O_3 enhancement over Hong Kong is as a result of transport of photochemical O_3 produced from biomass burning emissions from the upwind SE Asian continent. The large-scale enhancements of O_3 in tropical SE Asia and the subtropical western Pacific rim that result from SE Asian biomass burning activities such as presented here thus are of atmospheric importance and deserve further research efforts. *INDEX TERMS*: 0305 Atmospheric Composition and Structure: Aerosols and particles (0345, 4801); 0345 Atmospheric Composition and Structure: Pollution—urban and regional (0305); 0365 Atmospheric Composition and Structure: Troposphere—composition and chemistry; 0368 Atmospheric Composition and Structure: Troposphere—constituent transport and chemistry; *KEYWORDS*: tropospheric ozone, biomass burning emissions, pollutant transport

Citation: Chan, C. Y., L. Y. Chan, J. M. Harris, S. J. Oltmans, D. R. Blake, Y. Qin, Y. G. Zheng, and X. D. Zheng, Characteristics of biomass burning emission sources, transport, and chemical speciation in enhanced springtime tropospheric ozone profile over Hong Kong, *J. Geophys. Res.*, 108(D1), 4015, doi:10.1029/2001JD001555, 2003.

¹Department of Civil and Structural Engineering, Hong Kong Polytechnic University, Hong Kong, China.

²NOAA Climate Monitoring and Diagnostics Laboratory, Boulder, Colorado, USA.

³Chemistry Department, University of California, Irvine, California, USA.

⁴Department of Atmospheric Sciences, School of Physics, Peking University, Beijing, China.

⁵Chinese Academy of Meteorological Sciences, Beijing, China.

1. Introduction

[2] Biomass burning emissions associated with natural and human activated fires are an important source of O_3 and its precursors [Crutzen *et al.*, 1979; Andreae *et al.*, 1994; Lelieveld *et al.*, 2001]. Fishman *et al.* [1992] proposed that biomass burning emissions could affect tropospheric ozone on hemispheric and global scales due to long-range transport processes. Tropical Southeast (SE) Asia is an active biomass-burning region as a result of increasing deforesta-



Figure 1. Map showing the geographical locations of Hong Kong and selected Southeast Asia countries. A, B, and C are the locations where the altitudinal profile data were obtained by the DC-8 aircraft.

tion and agricultural activities [Stott, 1988; Christopher and Kimberly, 1996]. Dwyer *et al.* [1988] identified mainland SE Asia and the Orissa Province in eastern India as regions of very high active fire concentration. Christopher and Kimberly [1996] have identified east-central India and the region containing Thailand, Laos, Cambodia and Vietnam as the two major areas of biomass burning in India and SE Asia. There has been significant progress in the monitoring of forest fires in the Indonesian region [Thomas *et al.*, 1998; Lelieveld *et al.*, 2001; Thompson *et al.*, 2001] and the understanding of their impacts on the atmospheric environment [Fujiwara *et al.*, 1999; Tsutsumi *et al.*, 1999; Chan *et al.*, 2001]. However, the effects of the emissions from large-scale fires in mainland SE Asia are less well known compared with those in most other regions such as Africa and South America [Folkins *et al.*, 1997; Christopher *et al.*, 1998].

[3] Tropospheric O₃ over Hong Kong has been measured since 1993. Liu *et al.* [1999] reported high O₃ events in the lower troposphere in spring 1996. The authors speculated on the possible relationship of the high O₃ levels with biomass burning activities in SE Asia. Chan *et al.* [2000] showed that the O₃ enhancement observed in spring 1994 over Hong Kong is related to photochemistry and transport of O₃ precursor-rich air that originated from biomass burning emissions from the Indo-Burma region of the SE Asia continent. Chan *et al.* [2001] reported substantial O₃ enhancements over many parts of tropical SE Asia and the subtropical south China region including Hong Kong in midautumn and early winter (October–December) of 1997, when many forest fires occurred in the Indonesian region. In this case, O₃ enhancements were caused by the large-scale outflows of O₃ and other pollutants from the Indonesian region and were related to the abnormal atmospheric meteorological conditions that associated with the strong El Niño phenomenon. Such O₃ enhancements were estimated to cause substantial changes in the atmospheric radiative

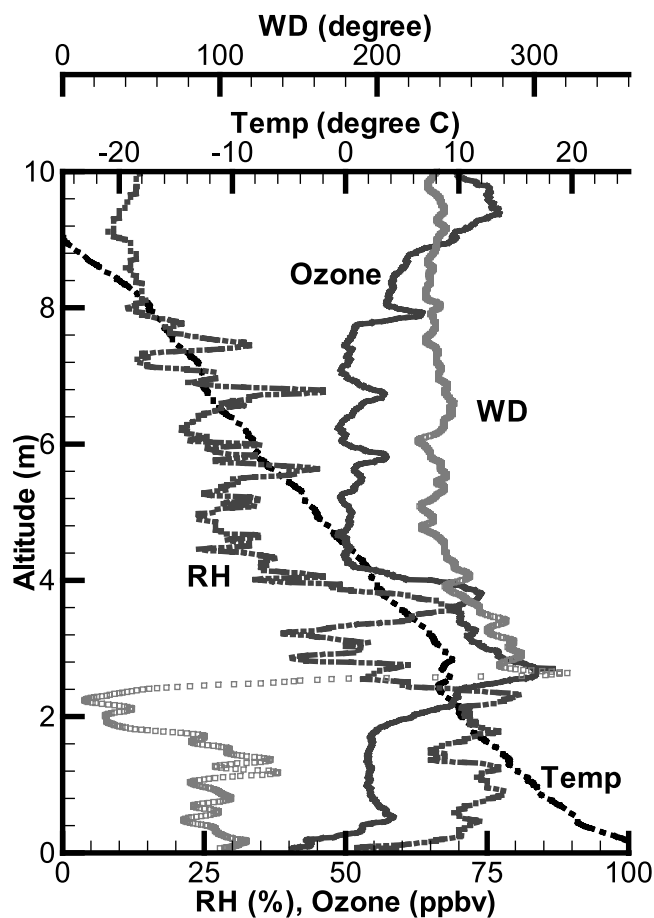


Figure 2. Ozone, temperature, relative humidity (RH) and wind direction (WD) profiles of a typical ozone enhancement event over Hong Kong (March 3, 1999).

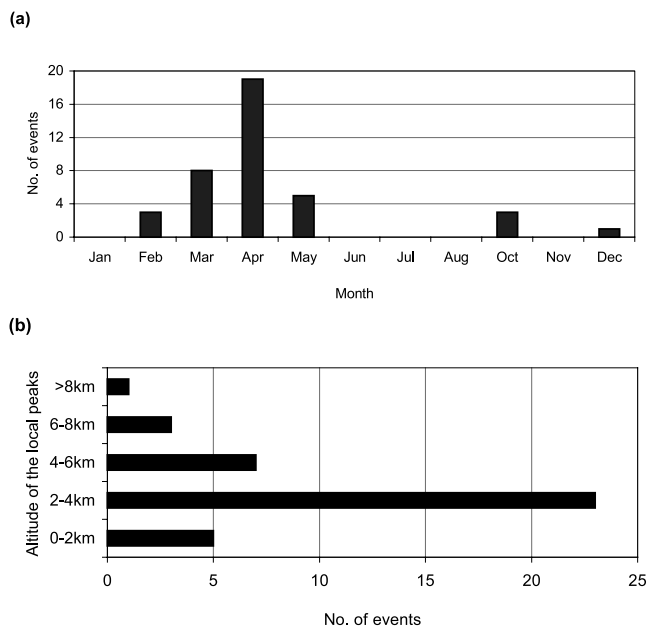


Figure 3. (a) Seasonal distribution of ozone enhancement events over Hong Kong, and (b) the vertical distribution of the local ozone peaks.

forcing and surface temperature elevation in the Hong Kong region [Chan *et al.*, 2001].

[4] We continued to observe O_3 enhancement events over Hong Kong in our new experiment period from 1997 to 1999. In this paper, we further study these events using the 6-year ozonesonde data from 1993 to 1999. The aim is to establish the seasonal variation of these events and assess their relation to the springtime O_3 maximum in the lower troposphere over Hong Kong. The chemical and transport characteristics and biomass burning emission sources of O_3 -rich air mass in the enhanced O_3 profile will be examined

using ozonesonde, satellite image and valuable trace gas data measured on board the DC-8 aircraft during the PEM-West-B experiment.

2. Experiment and Method

2.1. Ozone Sounding

[5] The vertical O_3 profile over Hong Kong is measured by an electrochemical concentration cell (ECC) balloon-borne ozonesonde [Komhyr, 1995] together with simultaneous pressure, temperature, dew point, relative humidity (RH) and wind measurements by Vaisala radiosonde. The sounding data is recorded by a Vaisala DigiCORA system. Chan *et al.* [1998b] has described the detailed measurement methodology, and quality control procedures for each O_3 profile. The ozonesonde was launched at the Hong Kong Observatory King's Park Meteorological Station, which is located in an urban area 66 m above mean sea level. Each experiment was performed at 0530 UTC (1330 local time) from October 1993 to September 1999. A total of 180 O_3 profiles were available for this study. There were 4, 19, 23, 91, 24, 9 and 10 profiles from 1993 to 1999, respectively. There was at least one O_3 profile per month during this period, with exceptions in November 1993, June 1997, July, September and October 1998, and July and August 1999. More O_3 profiles were obtained in winter (December to February) and spring (March to May), when we frequently observed O_3 enhancement and depletion events. During the intensive study period from November 1995 to April 1997 there was at least one profile per week.

2.2. Air Trajectories

[6] Backward and forward air trajectories from the NOAA Climate Monitoring and Diagnostics Laboratory were used in this study. The trajectories were calculated by the model described by Harris and Kahl [1994]. The model calculates 10-day air trajectories using input data from the European Centre for Medium Range Weather Forecasts and National Meteorological Centre of the United

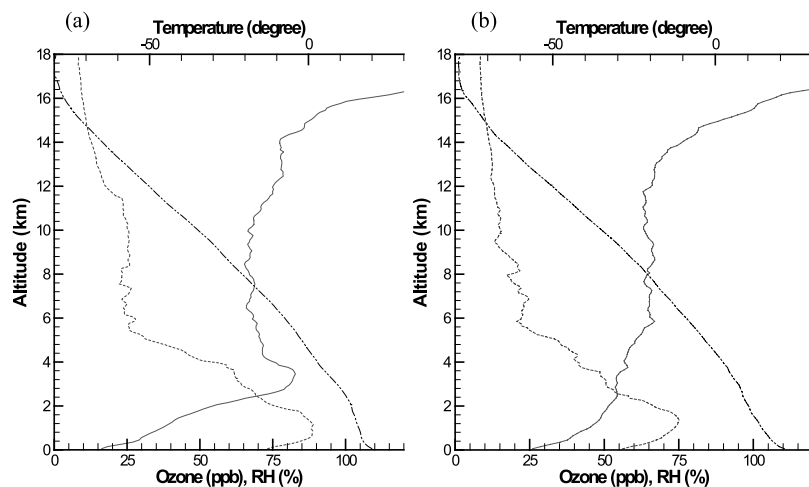


Figure 4. Average ozone (solid line), temperature (dash-dotted line) and relative humidity (dotted line) profiles for (a) enhancement cases and (b) nonenhancement cases for the period October 1993 to September 1999.

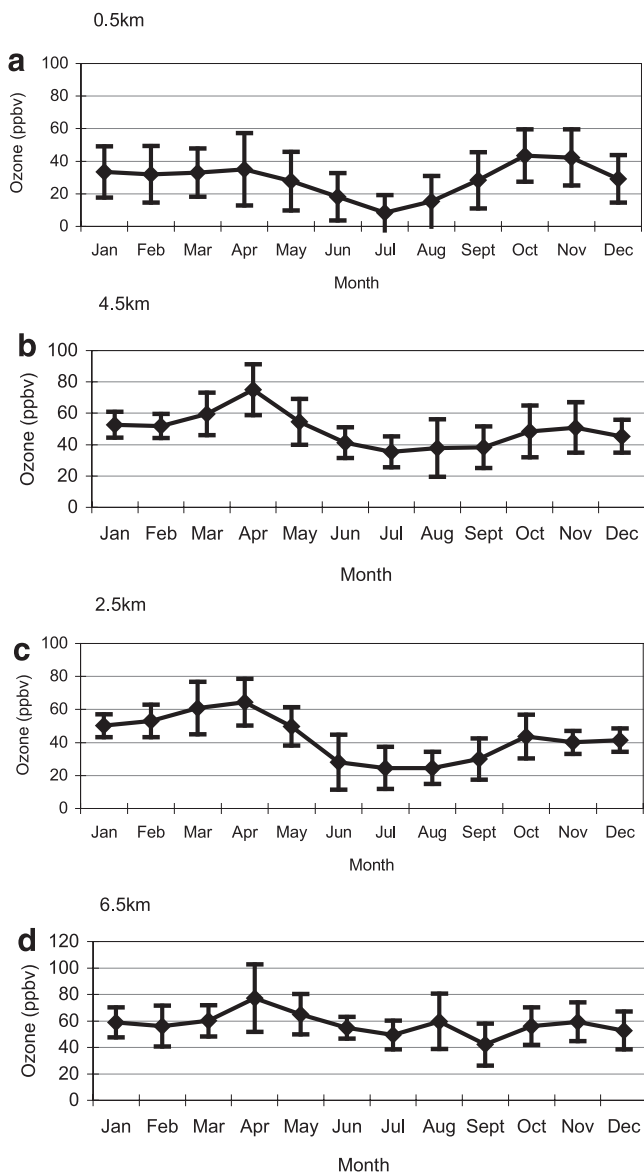


Figure 5. Seasonal distribution of ozone at (a) 0.5, (b) 2.5, (c) 4.5 and (d) 6.5 km over Hong Kong for the period October 1993 to September 1999. The error bars show one standard deviation.

States. The data have a spatial resolution of 2.5 degree and a temporal resolution of 12 hours. Each trajectory is produced together with altitude, pressure and temperature at each point. In this model, an air parcel is assumed to move dry adiabatically along a given isentropic surface. The modeled trajectories are believed to give a reasonable representation of large-scale circulation. They can be used to examine potential source regions of pollutants although the exact origin of a specific air parcel cannot be determined. Trajectories of this kind have been applied previously to document the climatology of atmospheric motion [Oltmans *et al.*, 1996; Harris *et al.*, 1998]. In this study, two daily trajectories at 0000 and 1200 UT were calculated at the standard pressure levels and altitudes of interest for each O_3 profile.

2.3. Satellite Images of Fire Count

[7] We used the fire count data from the European Space Agency (ESA) to identify the biomass burning activity in the SE Asia region. The fire counts were extracted from the Along Track Scanning Radiometer (ATSR) World Fire Atlas (European Space Agency, ATSR World Fire Atlas, available at <http://shark1.esrin.esa.it/ionia/FIRE/AF/ATSR>), and were derived from data obtained by the optical ATSR sensor on board the European ERS-2 satellite. The ATSR instrument has a spatial resolution of $1 \times 1 \text{ km}^2$. In this study, we focused on the sampling region from 70°E to 130°E , and from -10°N to 30°N . Figure 1 shows the geographical locations of the countries within the region. A detailed description of the fire detection algorithm for the ATSR data, including advantages and limitations of the derived data, is available at the ESA website (<http://shark1.esrin.esa.it/ionia/FIRE/AF/ATSR>).

2.4. Chemical Measurements During PEM-West B

[8] We used the trace gas measurements on board the research aircraft (DC-8) during the NASA's 1994 PEM-West B campaign to assess the chemical characteristics of O_3 -rich air masses reaching Hong Kong. Hoell *et al.* [1997] and references therein have detailed the measurement characteristics such as sampling techniques, averaging times, and accuracy. In particular, we are interested in the altitudinal profile data obtained during ascents and descents of the aircraft close to the subtropical region of south China on February 21, 25 and 27, 1994. The data represents 10-s average values. The profile data cover the regions from 15.91°N , 117.38°E to 15.91°N , 117.4°E on February 21, 1994, from 21.53°N , 115.01°E to 22.45°N , 114.26°E and 117.2°E to 117.2°E and 8.8°N to 22.4°N on February 25, 1994, and from 24.8°N , 120.57°E to 22.52°N , 119.83°E on February 27, 1994.

3. Results and Discussion

3.1. Enhanced Springtime Ozone Profiles Over Hong Kong

[9] We have been continuously observing O_3 enhancement in the lower troposphere over Hong Kong since middle February 1994. Figure 2 shows O_3 , temperature, relative humidity (RH) and wind profiles of a typical O_3 enhancement, in this case observed in March 1999. In general, the O_3 enhancements feature an O_3 -rich layer overlying the boundary layer in the lower and middle troposphere with the O_3 peak at lower elevations (2.5–4.0 km). These O_3 -rich layers are usually 2–4 km thick and are characterized by moderate to high RH (50 to 100%). They are isolated from the local boundary layer (BL) influence by a temperature inversion at the bottom of the O_3 layer, where a sharp decrease in RH also occurred. The O_3 -rich air masses are always accompanied by a westerly wind. We also observed O_3 enhancements at higher altitudes less frequently. The moderate RH observed simultaneously with the O_3 -rich air masses confirms that the O_3 was not of stratospheric origin. Stratospheric air rich in O_3 is expected to be dry in nature and with comparatively low RH [Johnson and Viezee, 1981]. On the other hand, the strong temperature inversion at the bottom of the O_3 -rich air mass indicated that the air masses were rela-

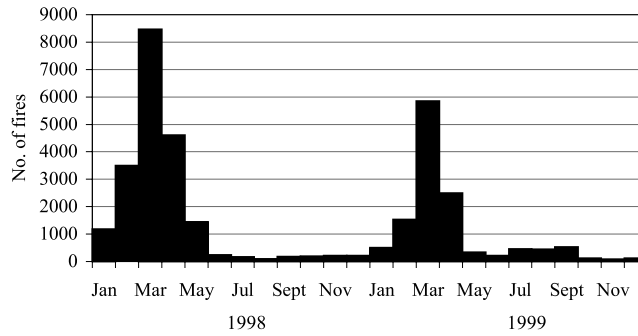


Figure 6. Seasonal distributions of fires in Southeast Asia (-10°N to 30°N , 70°E to 130°E) in 1998 and 1999.

tively isolated from the O_3 produced from emission sources in the local BL. These facts lead us to believe that the elevated O_3 was horizontally transported from distant sources.

[10] We have utilized the O_3 , temperature, and RH profiles, to identify 39 O_3 enhancement events in our data set from 1993 to 1999. The selection criteria of the events are as follows: (1) the O_3 -enhanced layer occurred between

the BL (below 2 km) and the middle troposphere (10 km) with a local peak O_3 concentration greater than 75 ppbv, and (2) the corresponding RH value at this local O_3 peak is greater than 50%. The use of these criteria is arbitrary but with reference to the average profile of the nonenhancement events. Figure 3 shows the seasonal distribution of the O_3 enhancement events and the vertical distribution of the local O_3 peaks. Surface enhancement events are also shown

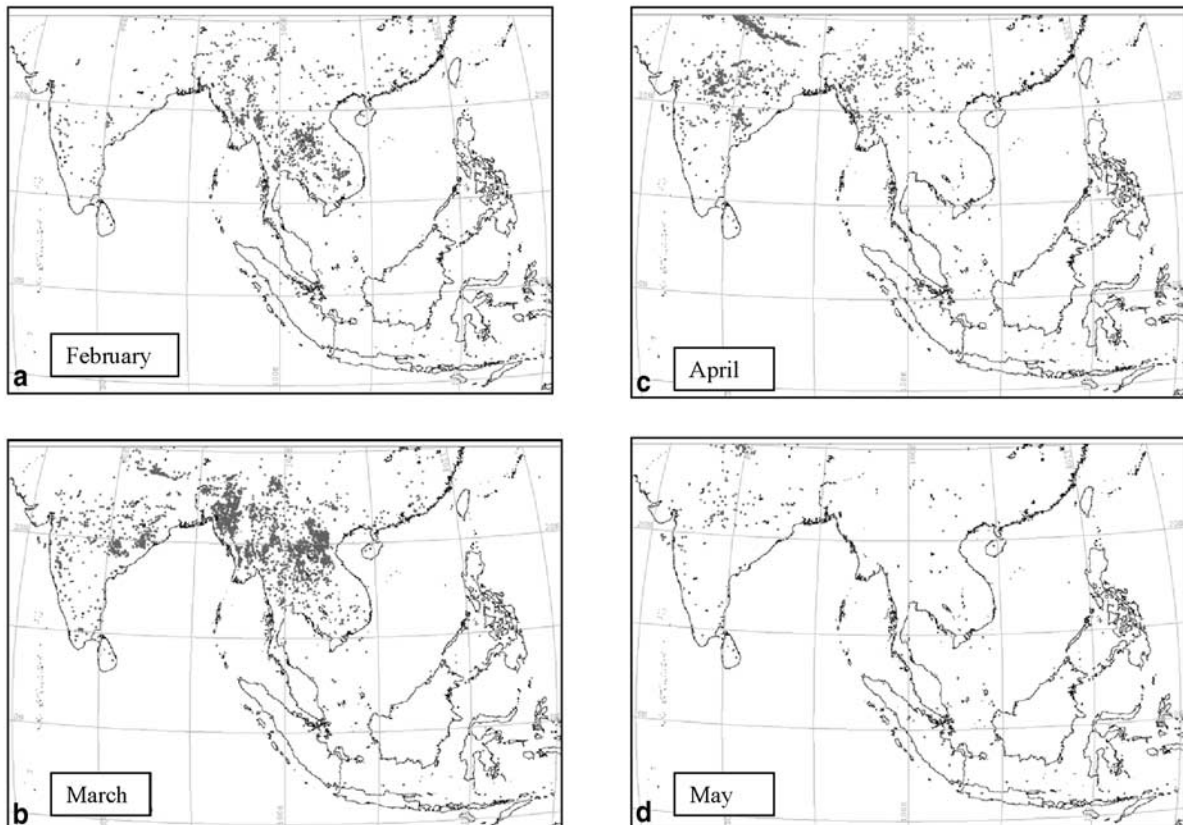


Figure 7. Geographical distributions of fires in Southeast Asia (-10°N to 30°N , 70°E to 130°E) from (a) February, (b) March, (c) (April) and (d) May 1999. The fire locations at a resolution of $1 \times 1 \text{ km}^2$ are denoted in red.

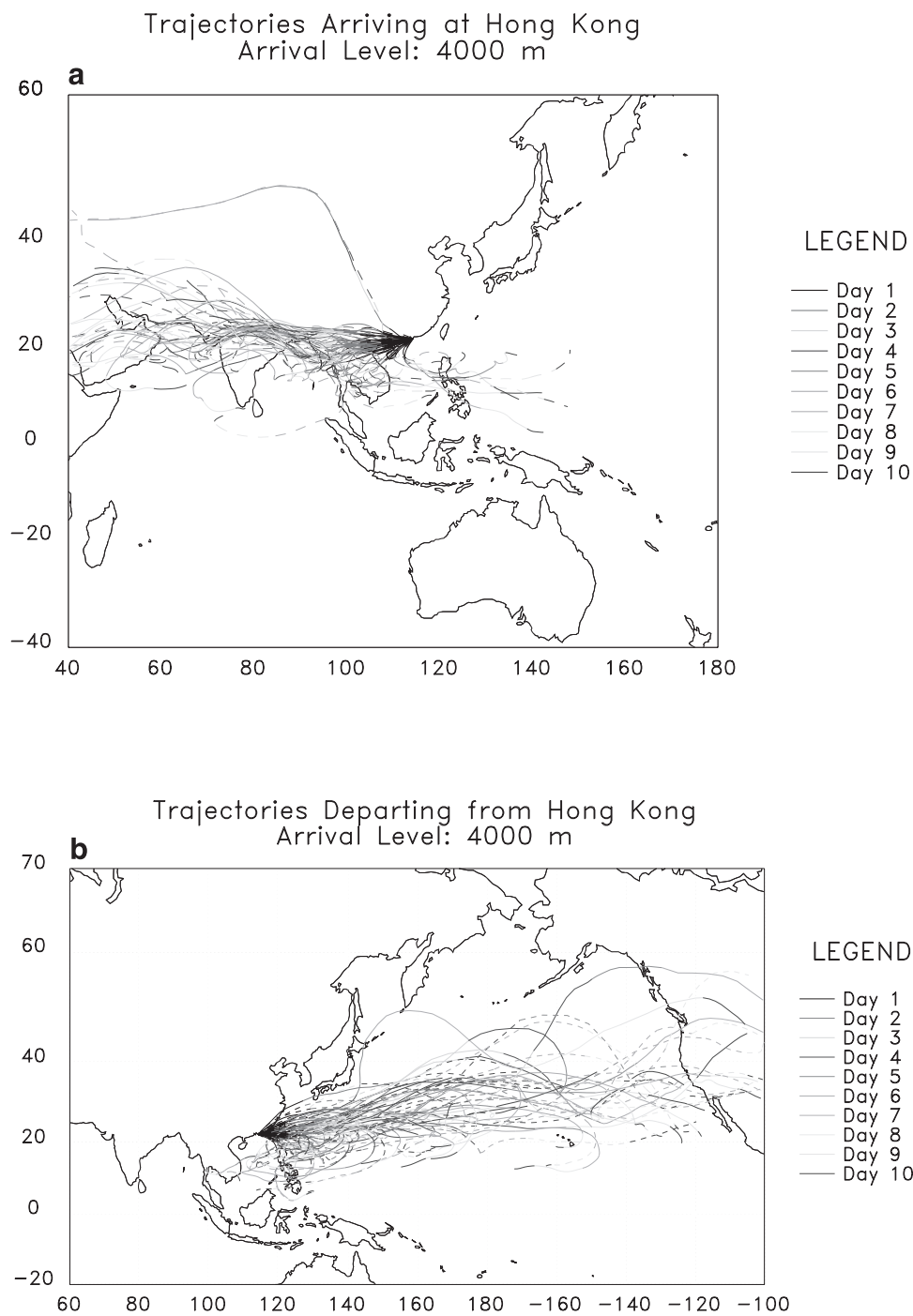


Figure 8. Ten-day (a) backward air trajectories reaching Hong Kong, and (b) forward trajectories departing from Hong Kong at 4 km during the ozone enhancement events from October 1993 to September 1999.

for comparison. A total of 35 cases occurred from late February to May with the majority occurring in spring (March to May), which accounted for 74% of the total number of profiles obtained from February to May (47). A few cases of BL (<2 km) O₃ enhancement occurred in October (3) and December (1). The tropospheric O₃ enhancement events in October and December 1997 reported by Chan *et al.* [2001] are not included because they do not fulfil the selection criteria. Most of the local O₃

peaks were concentrated between 2–4 km (23 cases). There were some cases (7) at the 4–6 km altitude. The total number of cases within the 2.0–6.0 km altitude range accounted for 77% of the total number of O₃ events. The peak O₃ concentrations exceeded 100 ppbv in 12 of the cases. The maximum O₃ concentration recorded between 1993–1999 was 138 ppbv at 3.1 km.

[11] The excess O₃ in the O₃-rich layers adds substantially to the tropospheric O₃ mixing ratios and noticeably

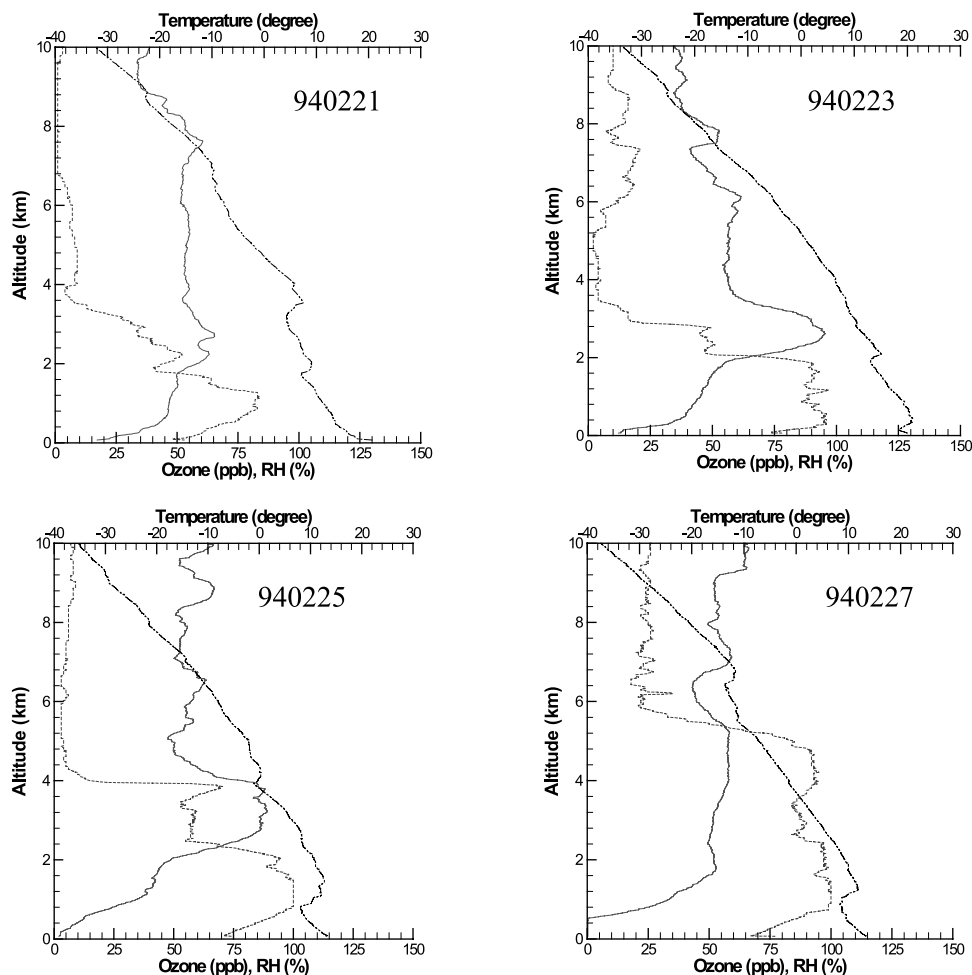


Figure 9. Ozone (solid line), temperature (dash-dotted line) and relative humidity (dotted line) profiles over Hong Kong from February 21 to 27, 1994. (a) February 21; (b) February 23; (c) February 25; and (d) February 27.

modifies the average O_3 profile and results in an overall springtime O_3 maximum in the lower troposphere. Figure 4 shows the average profiles of O_3 , relative humidity and temperature for the enhancement and nonenhancement cases. The enhanced O_3 profiles were characterized by a sharp peak in the lower troposphere, especially at altitudes between 2.5 to 4.0 km. Accompanying the O_3 enhancement, relative humidity also showed higher values. We also compared the tropospheric O_3 column (TOC) for the O_3 enhancement and nonenhancement cases. The mean TOC for the enhancement cases is 48.3 DU, which exceeds the value of the nonenhancement cases by 12%.

[12] Figure 5 shows the distribution of O_3 mixing ratios at 0.5, 2.5, 4.5 and 6.5 km over Hong Kong by month for the period October 1993 to October 1999. These ratios represent the average values of approximately 8 data points centered at the altitudes. The error bars indicate ± 1 standard deviation. There were at least seven soundings per month that went into the monthly average. Ozone in the low and middle free troposphere, especially at 2.5 and 4.5 km, shows an increasing trend after January reaching a maximum in April. The O_3 maximum is not observed in April at 0.5 km. The springtime O_3 maximum in the lower and middle free troposphere over Hong Kong is similar in

timing to that over Hilo reported by *Oltmans et al.* [1996] and Mauna Loa Observatory by *Harris et al.* [1998].

3.2. Biomass Burning Activity in Southeast Asia

[13] The occurrence of springtime O_3 enhancement events over Hong Kong coincided with the dry season in the tropical SE Asian continent, where biomass burning is frequent, resulting from natural processes and human activities. Figure 6 shows the monthly distribution of fire counts in SE Asia for the years 1998 and 1999. The fire activity in 1998 and 1999 showed a distinct seasonal pattern with a gradual increase from January to March, when it reached a peak. It then decreased substantially from late spring (May) to a minimum in summer. In 1998 and 1999, there were over 20,500 and 12,700 hot spots of fire detected, respectively. During the O_3 enhancement period from February to May 1998 and 1999, there were a total of 18,000 and 10,200 fires detected, respectively. That is, more than 80% of the annual fire hot spots occurred between February and May.

[14] Figure 7 shows the geographical distribution of the monthly integrated fire hot spot map in the SE Asian region from February to May 1999. The most extensive fires were found in the Indo-Burma (Myanmar) region of the SE Asian

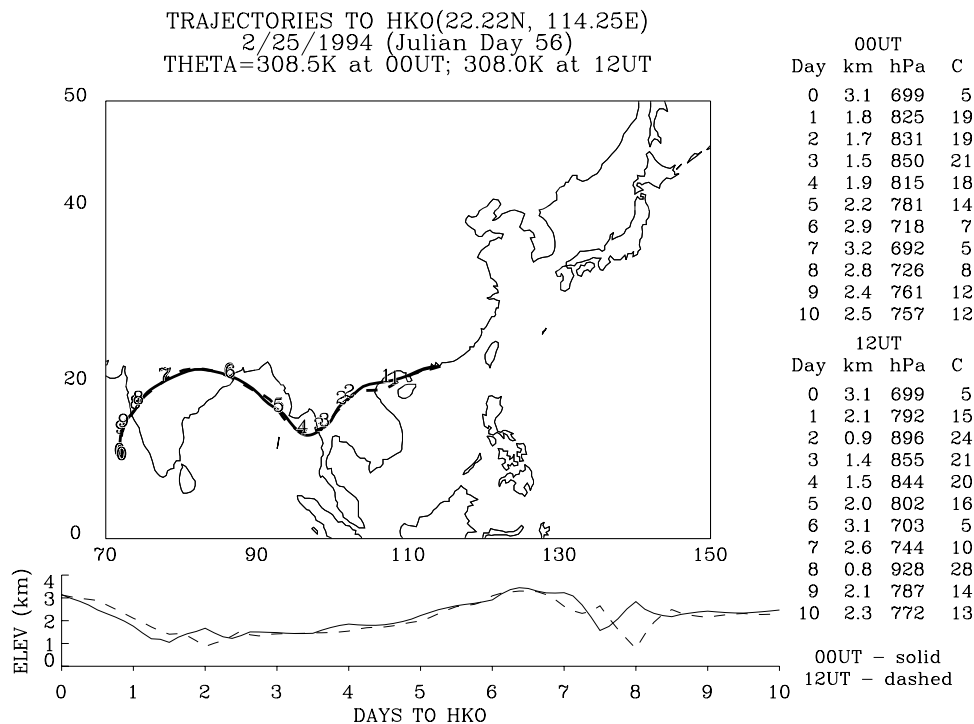


Figure 10. Backward air trajectories at 3.1 km on February 25, 1994. The solid line is for 0000 UT and the dashed line is for 1200 UT.

continent, especially in the surroundings of Burma, Laos and northern Thailand (Figure 7c) and northern India and Nepal of the Indian subcontinent (Figures 7b and 7c). The fire hot spots in south China, Philippine islands, Malaysian Peninsula and Indonesian regions were comparatively fewer. A substantial number of fire hot spots was also found from February to May 1997. However, the maximum fires in this year occurred in the Indonesian and, to a lesser extent, Malaysian regions (not shown) as a result of the strong El Niño phenomenon in that year.

[15] Based on the large number of fires recorded by the satellite images, it is reasonable to believe that very large amounts of O₃ precursors were emitted to the atmosphere over SE Asia from the biomass burning associated with the fires. Convective activity over the SE Asian continent begins in spring [Jacob et al., 1999]. This together with the strong thermal buoyancy and turbulence created by the active fires is able to carry pollutants to higher altitudes where they are carried downwind along the trajectories. In the following section, we will examine the transport characteristics of the O₃-rich air masses across the active fire regions in SE Asia by back air trajectory.

3.3. Transport Characteristics of Ozone-Rich Air Mass

[16] Figure 8a shows 10-day backward air trajectories arriving at Hong Kong at 4 km altitude for the O₃ enhancement cases from 1993 to 1999. This altitude is the location where most local O₃ peaks were found. The trajectories at 4, 5 (not shown), and 6 km (not shown) indicate that the air masses originated from as far as the vicinity of the Mediterranean Sea in 10 days. They travelled through the north India, Indo-Burma and Indo-China region before reaching China. The trajectories at 3.0 km show that the air masses spent more time over the Indo-

China regions of the SE Asian continent before reaching the south China region. Some cases show that the air masses came from the western Pacific over the vicinity of the Philippine Islands and then travelled over the Indo-China region, and the South China Sea before reaching south China and Hong Kong. In one case, the air masses originated from the central Asian continent. All the trajectories show that the O₃-rich air masses spent some time traveling across the region where active biomass burning activities were found. The region included the Indian peninsula, and the Indo-Burma and Indo-China region of the SE Asian continent.

[17] Figure 8b presents the 10-day forward air trajectories at 4 km for all the O₃ enhancement cases departing from Hong Kong. The trajectories show that most of the O₃-rich air masses passed through the southeast Chinese coast to the western and central Pacific in a general northeast direction across Taiwan Island and southern Japan. In some cases, the air masses turned clockwise after departing from the Asian coast and moved southwards to the tropical region over the vicinities of the Philippine islands and the South China Sea. The trajectories show that the O₃-rich air masses can reach the central Pacific in 2–6 days. The trajectories also indicate that in many cases the O₃-rich air masses traveling at higher altitudes (e.g., 4, 5 (not shown) and 6.0 km (not shown)) can reach the western coast of North America within 10 days.

3.4. Chemical Characteristics of Ozone-Rich Air Masses: A Case Study During the PEM-West B Period

[18] During the PEM-West B mission, which deployed in late winter from February 21 to 27, 1994, ozonesondes were launched every 2 days, and O₃ enhancements were observed over Hong Kong (Figure 9). In this event, a small O₃-rich layer was first observed on February 21 from 2.0 to 4.0 km

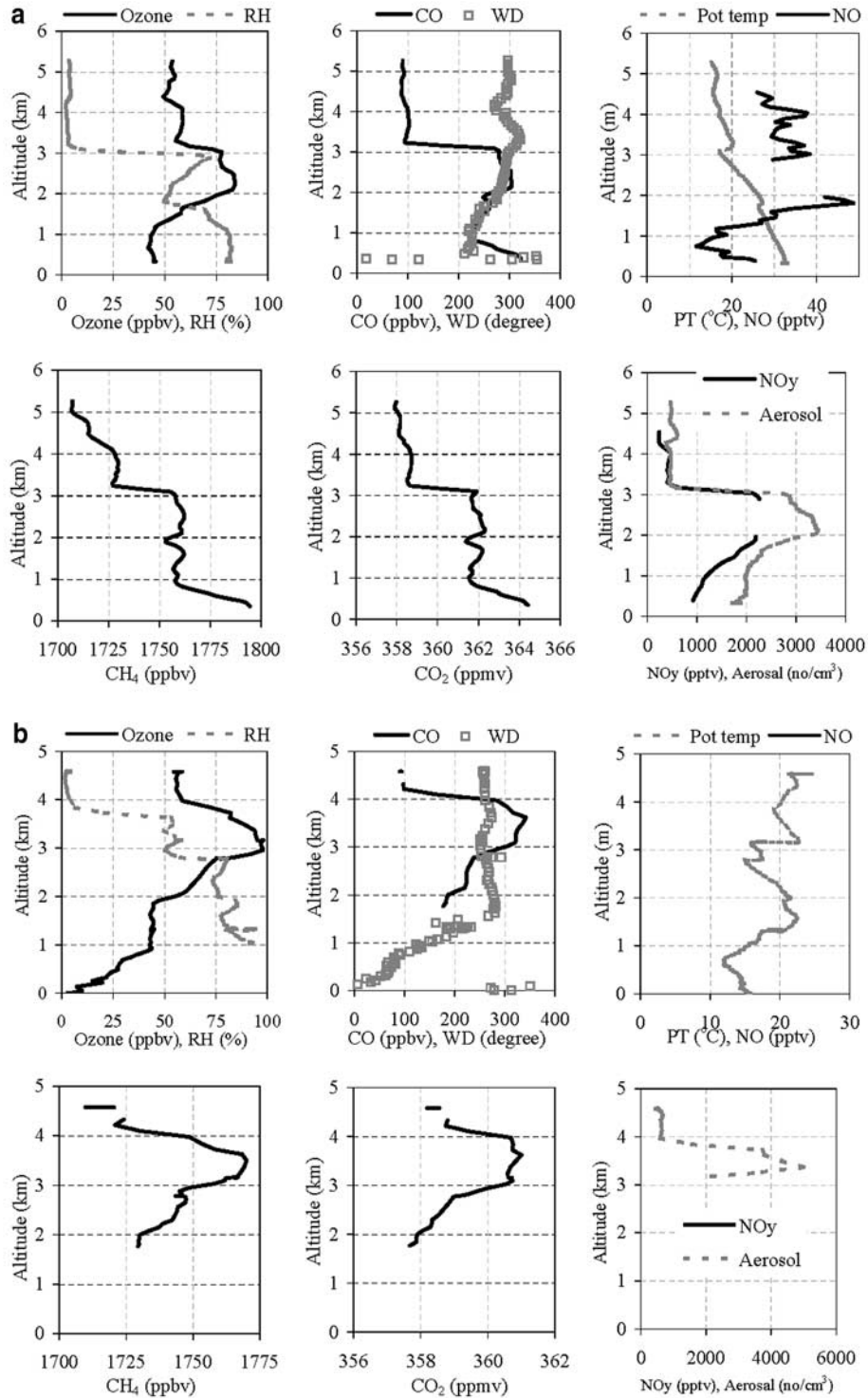


Figure 11. Vertical profiles of ozone, aerosol density, carbon monoxide (CO), nitrogen oxide (NO), total nitrogen oxidants (NO_y), methane (CH₄), carbon dioxide (CO₂), potential temperature (PT), relative humidity (RH), and wind direction (WD) over (a) the western Philippines on February 21, 1994, (b) the Hong Kong region on February 25, 1994 and (c) the western Pacific Ocean on February 27, 1994.

with a maximum O₃ concentration of 65 ppbv. The peak O₃ concentration reached a maximum of 98 ppbv on February 23, and had decreased to 88 ppbv by February 25. The peak then subsided to around 50 ppbv on February 27. Figure 10 shows the backward air trajectories to Hong Kong at the

altitude of the O₃ peak at 3.1 km (699 hPa) for 00UT and 12 UT on February 25. The trajectory shows that the O₃-rich air masses originated over the eastern Arabian Sea and traveled through the region close to the northern India, Nepal and Bangladesh. They then traveled over the Bay of Bengal in

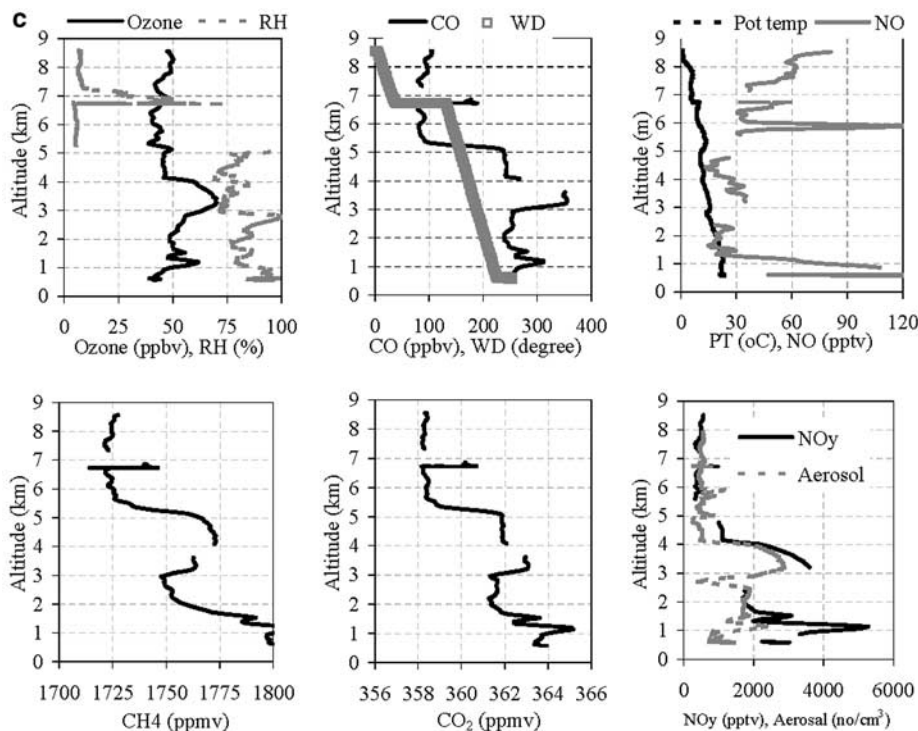


Figure 11. (continued)

the vicinity of Indo-Burma and the Indo-China region including northern Thailand, Laos and northern Vietnam to south China and Hong Kong. Note that these regions are the active biomass burning region, where most fire hot spots were found (Figure 7).

[19] The DC-8 aircraft flew across the tropical and subtropical western Pacific on February 21, 25 and 27. Enhanced O₃ layers were also recorded by measurements on board the aircraft over the lower troposphere at various tropical and subtropical latitudes of the western Pacific. Figures 11a–11c show the vertical profiles of O₃, aerosol density, CO, NO, NO_y, CH₄, CO₂, potential temperature, RH and wind direction over tropical western Philippines (marked A in Figure 1) on February 21, subtropical Hong Kong (marked B in Figure 1) on February 25 and western Pacific Ocean (marked C in Figure 1) on February 27. On February 25, the enhanced O₃ layer (with a peak concentration of 98 ppbv at 2.9 km) was observed from 2.7 to 3.8 km altitudes over Hong Kong. On February 21 and 27, the peak concentrations were 84 ppbv at 2.2 km and 71 ppbv at 3.2 km over tropical eastern Philippines and western Pacific, respectively. The O₃-rich air masses were transported by a westerly wind and accompanied by a high RH of roughly 50%. They were also relatively isolated from air in the BL below by temperature inversions indicated by the noticeable changes in potential temperature at the bottom of the layers. Based on these observations, especially on February 25 over the Hong Kong region, it is reasonable to assume that the O₃-rich air masses captured by measurements on board the DC-8 aircraft are similar to those observed by ozonesonde over Hong Kong.

[20] Figure 12 shows the vertical profiles of ethyne (C₂H₂), ethane (C₂H₆), CH₃Cl and methyl bromide

(CH₃Br), which are emitted during biomass burning [Blake *et al.*, 1996], and C₂Cl₄, a tracer of urban pollution [McNeal *et al.*, 1998], over the latitude range from 8.8 to 22.4°N at 117.2°E longitude on February 25 including an altitudinal profile directly over Hong Kong. There were strong enhancements in C₂H₂, C₂H₆, CH₃Cl and CH₃Br at the altitudes of the elevated O₃, but there was no obvious enhancement of the urban pollution tracer, C₂Cl₄. In fact, the concentration of CH₃Cl, a biomass burning tracer, at the elevated O₃ altitude was even higher than that in the BL suggesting that we observed a biomass burning plume.

[21] Enhanced concentrations of trace gases were also found in these layers. In fact, the peak O₃ concentrations coincided with the peak trace gas concentrations. Table 1 summarizes the peak, median and standard deviation of concentrations of O₃, CO, nitrogen oxide (NO), total nitrogen oxides (NO_y), CH₄ and CO₂ in the O₃-enhanced layers. The peak CO concentrations on February 21, 25, and 27 were 305, 343, and 356 ppbv, respectively. The CO concentration over Hong Kong on February 25 was close to the concentration measured at the rural area in the BL [Chan *et al.*, 1998a]. The corresponding CO₂ concentrations were 362, 361, and 361 ppmv. The peak NO concentrations on February 21, and 27 were 47 and 36 pptv respectively. The corresponding NO_y concentrations were 2262 and 3603 pptv respectively. There was no NO and NO_y data on February 25. Photochemical O₃ production and destruction depend on the availability of the precursors, namely non-methane hydrocarbons (NMHCs), CH₄, CO, and nitrogen oxides (NO_x), and sunlight. Net O₃ production prevails when there are enough precursors and when the NO mixing ratio is higher than ~30 pptv [Crutzen, 1973; Fishman *et*

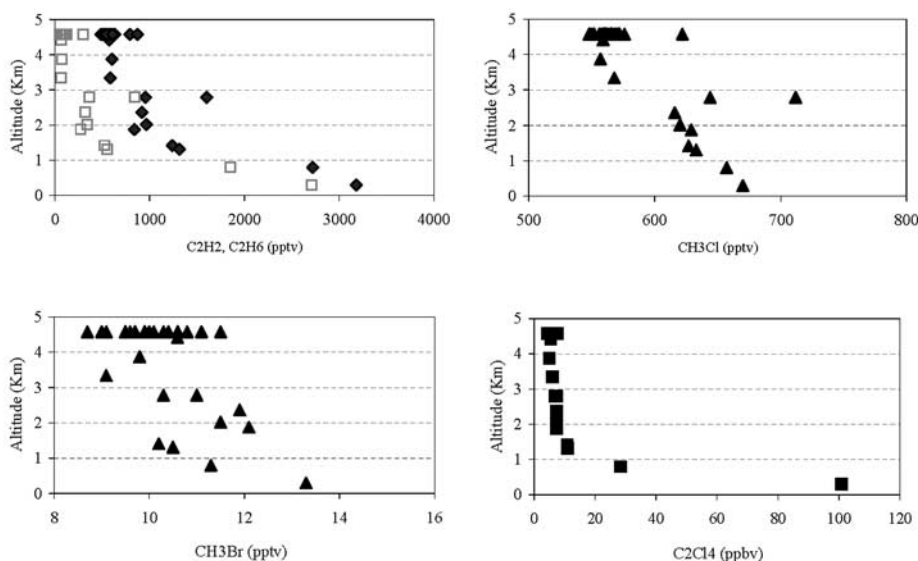


Figure 12. Vertical profiles of ethyne (C_2H_2), ethane (C_2H_6), methyl chloride (CH_3Cl), methyl bromide (CH_3Br) and carbon tetrachloride (C_2Cl_4) over $117.2^\circ E$ to $117.2^\circ E$ and $8.8^\circ N$ to $22.4^\circ N$ on February 25.

al., 1979]. The chemical trace gas measurements from the DC-8 aircraft suggest that the precursor levels associated with our O_3 -rich air masses provided enough O_3 precursors for net ozone production to occur through chemical mechanisms and photochemistry involving nitrogen oxides and hydrocarbons and/or the CO-OH- CH_4 cycle [Sze, 1977].

[22] Table 2 summarizes selected trace gas ratios, which were calculated based on the median trace gas concentrations in the O_3 enhancement layers of the profiles on February 21, 25 and 27. The gas ratios in the O_3 -rich air masses showed relatively small variability. The O_3/CO , O_3/CO_2 , CH_4/CO , CO/CO_2 and CH_4/CO_2 ratios over the Hong Kong region (marked A in Figure 1) were 0.3 (ppbv/ppbv), 0.2 (ppbv/ppmv), 6.2 (ppbv/ppbv), 0.8 (ppbv/ppmv) and 4.9 (ppbv/ppmv). The respective ratios were 0.3, 0.3, 5.5, 0.9 and 4.9 over eastern Philippines (marked B in Figure 1) on February 21, and 0.2, 0.2, 5.0, 1.0 and 4.9 over the western Pacific Ocean (marked C in Figure 1) on February 27. The small variability indicates that the O_3 -rich air masses over these regions have similar chemical characteristics although the air masses were observed in three different days and in a

wide region downwind of SE Asia continent. These together with the simultaneous enhancement of CH_3Cl , the biomass burning emission tracer, suggest that there were large-scale enhancements of O_3 in tropical SE Asia and the subtropical western Pacific rim as a result of biomass burning activities in SE Asia during the period.

4. Conclusion

[23] In this paper, we studied the O_3 enhancement events over Hong Kong and assessed their relation to the spring-time O_3 maximum in the lower troposphere over Hong Kong using the 6-year ozonesonde data from 1993 to 1999. We identified the source regions of biomass burning emission, and established the chemical and transport characteristics of O_3 -rich air mass in the enhanced O_3 profiles using satellite image, air trajectory, ozonesonde, and trace gas data measured on board the DC-8 aircraft during the PEM-West-B experiment.

[24] We identified a total of 39 enhancement events, among which 35 events (90%) occurred from late February

Table 1. Concentrations of Trace Gases and Meteorological Parameters in the Ozone Enhancement Layer on Board the DC-8 Aircraft^a

Date of Observation	Altitudes of Enhancement	Potential Temp., °C	Relative Humidity, %	CO ₂ , ppmv	O ₃ , ppbv	CO, ppbv	CH ₄ , ppbv	NO _y , pptv	NO, pptv	
Feb. 21, 1994	1.9–3.0 km	Peak	27.0	72.1	362.3	84.6	305.1	1762.2	2261.5	46.5
		Median	22.1	57.4	361.9	78.5	284.5	1760.2	2187.1	36.7
		Stdev	3.3	14.9	0.3	3.9	17.0	2.8	325.9	6.0
		N	18	18	18	18	18	6	6	
Feb. 25, 1994	2.7–3.8 km	Peak	22.7	80.5	361.0	98.0	342.5	1770.0	NV	NV
		Median	17.4	56.2	360.7	94.1	320.9	1762.0	NV	NV
		Stdev	2.4	16.3	0.7	10.0	38.0	9.5	NV	NV
		N	24	24	24	24	24	NV	NV	
Feb. 27, 1994	3.0–4.0 km	Peak	15.8	84.7	360.7	70.1	355.5	1763.9	3602.9	35.4
		Median	14.4	75.0	360.2	66.6	349.4	1762.5	3167.0	31.4
		Stdev	1.4	4.0	0.2	3.2	35.1	5.9	399.3	3.8
		N	16	16	13	16	11	11	12	12

^aNV, no data available; N, number of observations.

Table 2. Trace Gas Ratios in the Ozone Enhancement Layers

	O ₃ /CO (ppbv/ppbv)	O ₃ /CO ₂ (ppbv/ppmv)	CH ₄ /CO (ppbv/ppbv)	CO/CO ₂ (ppbv/ppmv)	CH ₄ /CO ₂ (ppbv/ppmv)
21-Feb	0.3	0.2	6.2	0.8	4.9
25-Feb	0.3	0.3	5.5	0.9	4.9
27-Feb	0.2	0.2	5.0	1.0	4.9

to May and 30 events (77%) had O₃ enhancement in the O₃-rich layer lying within the 2.0–6.0 km altitude. The excess O₃ in the O₃-rich layers adds an additional 12% of O₃ in the troposphere and results in an overall springtime O₃ maximum in the lower troposphere. Forward trajectory analysis suggested that the O₃-rich air masses over Hong Kong can reach the central Pacific and the western coast of North America within 10 days. Ozone on board the DC-8 aircraft revealed that O₃-rich air masses are found over many parts of the tropical SE Asia and subtropical western Pacific regions. The accompanying trace gas measurements suggest that the O₃-rich air masses have similar chemical characteristics and are rich in biomass burning emission tracer, CH₃Cl, but not the general urban emission tracers. The O₃ enhancement is as a result of transport of photochemically produced O₃ from biomass burning emissions from the upwind SE Asian continent. We identified Burma, Laos and northern Thailand of the SE Asia subcontinent and northern India and Nepal of the Indian subcontinent as the most active regions of biomass burning emission.

[25] Our finding on the cause of the springtime O₃ maximum in the lower troposphere over Hong Kong is different from that in the middle latitudes of the Northern Hemisphere. At these latitudes, the springtime O₃ maximum is commonly attributed to the active O₃ intrusion from the stratosphere and/or photochemical O₃ buildup from urban and industrial emissions in spring [Danielsen, 1968; Oltmans and Levy, 1992; Liu et al., 1987; Penkett and Brice, 1986; Kajii et al., 1998]. The large-scale enhancements of O₃ in the tropical SE Asia and subtropical western Pacific regions as a result of biomass burning activities in SE Asia such as presented here, thus are of atmospheric importance and deserve further research efforts.

[26] **Acknowledgments.** This study is supported by grants (PolyU 5037/98E, PolyU 5061/99E) from the Research Grant Council of Hong Kong, and an institutional research grant of The Hong Kong Polytechnic University (G-YW 58). The authors would like to acknowledge the contribution of the Hong Kong Observatory for the ozonesonde launching. The authors would like to acknowledge the European Space Agency for providing the fire count information. We thank the reviewers and Isobel Simpson for their helpful comments.

References

Andreae, M. O., B. E. Anderson, D. R. Blake, J. D. Bradshaw, J. E. Collins, G. L. Gregory, G. W. Sachse, and M. C. Shipham, Influence of plumes from biomass burning on atmospheric chemistry over the equatorial and tropical South Atlantic during CITE 3, *J. Geophys. Res.*, **99**, 12,793–12,808, 1994.

Blake, N. J., D. R. Blake, B. C. Sive, T.-Y. Chen, F. S. Rowland, J. E. Collins Jr., G. W. Sachse, and B. E. Anderson, Biomass burning emissions and vertical distribution of atmospheric methyl halides and other reduced carbon gases in the South Atlantic region, *J. Geophys. Res.*, **101**, 24,151–24,164, 1996.

Chan, C. Y., L. Y. Chan, S. Christopher, J. M. Harris, and S. J. Oltmans, The effects of 1997 Indonesian forest fires on tropospheric ozone enhancement, radiative forcing and temperature change over the Hong Kong region, *J. Geophys. Res.*, **106**, 14,875–14,885, 2001.

Chan, L. Y., C. Y. Chan, and Y. Qin, Surface Ozone Pattern in Hong Kong, *J. Appl. Meteorol.*, **37**(10), 1151–1165, 1998a.

Chan, L. Y., H. Y. Liu, K. S. Lam, T. Wang, S. J. Oltmans, and J. M. Harris, Analysis of the seasonal behavior of tropospheric ozone at Hong Kong, *Atmos. Environ.*, **31**, 159–168, 1998b.

Chan, L. Y., C. Y. Chan, H. Y. Liu, S. Christopher, S. J. Oltmans, and J. M. Harris, A case study on the biomass burning in Southeast Asia and enhancement of tropospheric ozone over Hong Kong, *Geophys. Res. Lett.*, **27**(10), 1479–1483, 2000.

Christopher, D. E., and E. B. Kimberly, Survey of fires in Southeast Asia and India during 1987, in *Global Biomass Burning*, vol. 2, edited by J. Levine, pp. 663–670, MIT Press, Cambridge, Mass., 1996.

Christopher, S. A., J. Chou, R. M. Welch, D. V. Kliche, and V. S. Connors, Satellite investigations of fire, smoke, and carbon monoxide during April 1994 MAPS mission: Case studies over tropical Asia, *J. Geophys. Res.*, **103**, 19,327–19,336, 1998.

Crutzen, P. J., A discussion of the chemistry of some minor constituents in the stratosphere and troposphere, *Pure Appl. Geophys.*, **106–108**, 1385–1399, 1973.

Crutzen, P. J., L. E. Heidt, J. P. Krasnec, W. H. Pollock, and W. Seiler, Biomass burning as a source of atmospheric gases CO, H₂, N₂O, NO, CH₃Cl, and COS, *Nature*, **282**, 253–256, 1979.

Danielsen, E. F., Stratosphere-troposphere exchange based on radio-activity, ozone and potential vorticity, *J. Atmos. Sci.*, **25**, 502–518, 1968.

Dwyer, E., J.-M. Gregoire, and J. P. Malingreau, A global analysis of vegetation fires using satellite images: Spatial and temporal dynamics, *AMBIO*, **27**, 175–181, 1988.

Fishman, J., V. Ramanathan, P. J. Crutzen, and S. C. Liu, Tropospheric ozone and climate, *Nature*, **282**, 818–820, 1979.

Fishman, J., V. G. Brackett, and K. Fakhruzzaman, Distribution of tropospheric ozone in the tropics from satellite and ozonesonde measurements, *J. Atmos. Terr. Phys.*, **54**, 589, 1992.

Folkens, A. R., D. Chatfield, D. Baumgardner, and D. Proffitt, Biomass burning and deep convection in southeastern Asia: Results from ASHOC/MAESA, *J. Geophys. Res.*, **102**, 13,291–13,299, 1997.

Fujiwara, M., K. Kita, S. Kawakami, T. Ogawa, N. Komala, S. Saraspriya, and A. Auripto, Tropospheric ozone enhancements during the Indonesian forest fire events in 1994 and in 1997 as revealed by ground-based observations, *Geophys. Res. Lett.*, **26**(16), 2417–2420, 1999.

Harris, J. M., and J. D. W. Kahl, Analysis of 10-day isentropic flow patterns for Barrow, Alaska: 1985–1992, *J. Geophys. Res.*, **99**, 25,845–25,855, 1994.

Harris, J. M., S. J. Oltmans, E. J. Diugokencky, P. C. Novelli, B. J. Johnson, and T. Mefford, An investigation into the source of the springtime tropospheric ozone maximum at Mauna Loa Observatory, *Geophys. Res. Lett.*, **25**(11), 1895–1898, 1998.

Hoell, J. M., et al., The Pacific Exploratory Mission-West Phase B: February–March 1994, *J. Geophys. Res.*, **102**, 28,223–28,240, 1997.

Jacob, D. J., et al., Transport and chemical evolution over the Pacific (TRACE-P): A NASA/GTE aircraft mission, white paper prepared by the TRACE-P Planning Committee (TRACE-P), 1999. Transport and Chemical Evaluation over the Pacific (TRACE-P): An Aircraft Mission for GTE, report, NASA Goddard Space Flight Center, Greenbelt, Md., 1999. (Available at <http://www-as.harvard.edu/chemistry/trop/tracep/whitepaper/text.html>)

Johnson, W. B., and W. Viezee, Stratospheric ozone in the lower troposphere, I, Presentation and interpretation of aircraft measurements, *Atmos. Environ.*, **15**, 1309–1323, 1981.

Kajii, Y., K. Someno, H. Tanimoto, J. Hirokawa, H. Akimoto, T. Katsuno, and J. Kawara, Evidence for the seasonal variation of photochemical activity of tropospheric ozone: Continuous observation of ozone and CO at Haplo, Japan, *Geophys. Res. Lett.*, **25**, 3505–3508, 1998.

Komhyr, W. D., Electrochemical concentration cell ozonesonde performance evaluation during STOIC 1989, *J. Geophys. Res.*, **100**, 9231–9244, 1995.

Lelieveld, J., et al., The Indian Ocean Experiment: Widespread air pollution from South and Southeast Asia, *Science*, **291**, 1031–1036, 2001.

Liu, H. Y., W. L. Chang, S. J. Oltmans, L. Y. Chan, and J. M. Harris, On springtime high ozone events in the lower troposphere from SE Asian biomass burning, *Atmos. Environ.*, **33**, 2403–2410, 1999.

Liu, S. C., M. Trainer, F. C. Fehsenfeld, D. D. Parrish, E. J. Williams, D. W. Fahey, G. Hubler, and P. C. Murphy, Ozone production in the rural troposphere and the implications for regional and global ozone distributions, *J. Geophys. Res.*, **92**, 4191–4207, 1987.

McNeal, R. J., D. J. Jacob, D. D. Davis, and S. C. Liu, The NASA global tropospheric experiment: Recent accomplishments and future plans, *IGAC Newsl.*, **13**, June 1998.

Oltmans, S. J., and H. Levy II, Seasonal cycle of surface ozone over the western North Atlantic, *Nature*, **358**, 392–394, 1992.

Oltmans, S. J., D. J. Hofmann, J. A. Lathrop, J. M. Harris, W. D. Komhyr, and D. Kuniyuki, Tropospheric ozone during Mauna Loa Observatory

- Photochemistry Experiment 2 compared to long-term measurements from surface and ozonesonde observations, *J. Geophys. Res.*, *101*, 14,569–14,580, 1996.
- Penkett, S. A., and K. A. Brice, The spring maximum in photo-oxidants in the Northern Hemisphere troposphere, *Nature*, *39*, 655–657, 1986.
- Stott, P., The forest as Phoenix: towards a biogeography of fire in mainland South East Asia, *Geogr.J.*, *154*, 337–350, 1988.
- Sze, N. D., Anthropogenic CO emissions: Implications for the CO-OH-CH₄ cycle, *Science*, *195*, 673–675, 1977.
- Thomas, W., E. Hegels, S. Slijkhuis, R. Spurr, and K. Chance, Detection of biomass burning combustion products in Southeast Asia from backscatter data taken by the GOME spectrometer, *Geophys. Res. Lett.*, *25*(9), 1317–1320, 1998.
- Thompson, A. M., J. C. Witte, R. D. Hudson, H. Guo, J. R. Herman, and M. Fujiwara, Tropical tropospheric ozone and biomass burning, *Science*, *291*, 2128–2132, 2001.
- Tsutsumi, Y., Y. Sawa, Y. Makino, J. Jensen, J. Gras, and B. Ryan, Aircraft measurement of ozone, NO_x, CO and aerosol concentrations in biomass burning smoke over Indonesia and Australia in October 1997: Depleted ozone layer at lower altitude over Indonesia, *Geophys. Res. Lett.*, *26*(5), 595–598, 1999.
-
- D. R. Blake, Chemistry Department, University of California, 570 Rowland Hall, Irvine, CA 92697-2025, USA. (dblake@orion.oac.uci.edu)
- C. Y. Chan and L. Y. Chan, Department of Civil and Structural Engineering, Hong Kong Polytechnic University, Hung Hom, Hong Kong, China. (cececychan@polyu.edu.hk; celychan@polyu.edu.hk)
- J. M. Harris and S. J. Oltmans, NOAA Climate Monitoring and Diagnostics Laboratory, R/E.CGI, 325 Broadway, Boulder, CO 80305, USA. (Joyce.M.Harris@noaa.gov; Samuel.J.Oltmans@noaa.gov)
- Y. Qin and Y. G. Zheng, Department of Atmospheric Sciences, School of Physics, Peking University, Beijing 100871, China. (qinyu@pku.edu.cn; zhengyg@water.pku.edu.cn)
- X. D. Zheng, Chinese Academy of Meteorological Sciences, 46 Zhong Guancun South Street, Haidian, Beijing 100081, China. (zhengxd@cma.gov.cn)